D2-2-04 - Oral 12:15 - 12:30 hrs *(conf196a14)*	**Tunable, High-Repetition-Rate, Femtosecond Optical Parametric Oscillator in the Visible** *O.* ***Kokabee,*** *A.* ***Esteban-Martin,*** *M.* ***Ebrahim-Zadeh***	**112**
12:30 – 14:00	**Lunch**	

Session	**D2-3-Nonlinear Optical Devices**
Date	**Wednesday, 10 Dec 08**
Time	**14:00 - 15:30 hrs**
Session Chair	Jean-Jacques **Zondy**
Room	**Executive Seminar Room 4.2**

D2-3-01 – Invited 14:00 – 14:30 hrs *(conf196a38)*	**Advances in Ultrafast and Continuous-Wave Optical Parametric Oscillators** *Ebrahim-Zadeh* ***Majid***	**112**
D2-3-02 – Invited 14:30 – 15:00 hrs *(conf196a7)*	**$ZnGeP_2$ in High Power Optical Parametric Oscillators** *E.* ***Lippert,*** *H.* ***Fonnum,*** *G.* ***Rustad****, K.* ***Stenersen***	**112**
D2-3-03 – Invited 15:00 – 15:30 hrs *(conf196a21)*	**10-mJ Few-Cycle OPCPA at 1.5 µm** *O. D.* ***Mücke,*** *A.* ***Pugžlys,*** *P.* ***Dombi****, S.* ***Ališauskas****, V.* ***Smilgevičius,*** *N.* ***Forget,*** *J.* ***Pocius****, L.* ***Giniūnas,*** *R.* ***Danielius****, A.* ***Baltuška***	**112**
15:30 – 16:00	**Tea Break**	

POSTER SESSION

Date	**Wednesday, 10 Dec 08**
Time	**16:00 - 18:00 hrs**
Room	**Foyer**

PD-01 - Poster *(conf196a1)*	**Study of Negative Lensing Effect in Transparent Molecular Liquids by Femtosecond Laser Pulses** *Jaw-Luen* ***Tang,*** *Chen-Wei* ***Chen,*** *Yi-Ci* ***Lee****, Tai-Huei* ***Wei****, Chia-Ing* ***Chiu,*** *Jian-Neng* ***Wang,*** *Tzer-Hsiang* ***Huang***	**115**
PD-02 - Poster *(conf196a2)*	**Hydrophobic Surface Fabrication by Laser Micro-Patterning** *M.* ***Tang,*** *M. H.* ***Hong,*** *Y. S.* ***Choo***	**115**
PD-03 - Poster *(conf196a3)*	**Modeling a CW Single-Frequency Yb:Silica Fiber MOPA System and Determination the Gain and Saturation in the Optimum Length** *Parviz* ***Parvin,*** *Maryam* ***Ilchi-Ghazaani,*** *Alireza* ***Bananej****, Zohre* ***Lali-Dastjerdi***	**116**

10-mJ Few-Cycle OPCPA at 1.5 µm

O. D. Mücke[1], A. Pugžlys[1], P. Dombi[1], S. Ališauskas[2], V. Smilgevičius[2], N. Forget[3], J. Pocius[4], L. Giniūnas[4], R. Danielius[4], and A. Baltuška[1]

[1] Photonics Institute, Vienna University of Technology, Gusshausstr. 27-387, A-1040 Vienna, Austria

[2] Laser Research Center, Vilnius University, Saulėtekio av. 10, LT-10223 Vilnius, Lithuania

[3] Fastlite, Bâtiment 403, Ecole Polytechnique, 91128 Palaiseau, France

[4] Light Conversion Ltd., P/O Box 1485, Saulėtekio av. 10, LT-10223 Vilnius, Lithuania

***Abstract*- We report on a 4-stage OPCPA system for high-field applications delivering 10-mJ ~40-fs pulses at 1.5 µm. The system is based on a fusion of femtosecond DPSS Yb technology and a picosecond Nd:YAG pump laser. In a first preliminary filamentation experiment in xenon, we observe spectral broadening of the recompressed multi-mJ 1.5 µm pulses.**

I. INTRODUCTION

Optical Parametric Chirped-Pulse Amplification (OPCPA) [1] has attracted a lot of attention as a promising route toward intensity scaling of few-cycle laser pulses. Intense phase-stable few-cycle laser pulses have numerous intriguing applications in attosecond science and high-field science including attosecond XUV/soft-X-ray pulse generation by high-harmonic generation (HHG) [2-4], tomographic imaging of molecular orbitals [5], and laser-induced electron diffraction [6]. A major challenge for using HHG in studies of time-resolved tomography of molecular dissociative states is the low ionization potential I_p of excited molecular states. The resulting competition between state depletion and HHG prevents generation of broad HHG spectra necessary for tomographic reconstruction. One solution are laser sources with high ponderomotive energy $U_p \propto \lambda^2 I$ at moderate intensity level, i.e., infrared phase-stable few-cycle high-power laser systems. High-U_p-sources [7-9] also open the door to experimental investigations of the λ-scaling laws of strong-field physics [10,11] (Keldysh parameter $\propto\lambda^{-1}$, electron energies $\propto\lambda^2$, HHG cutoff $\propto\lambda^2$, HHG efficiency $\propto\lambda^{-5.5}$, minimum attosecond pulse duration $\propto\lambda^{-1/2}$), and they would benefit laser-induced electron diffraction because of the shorter de Broglie electron wavelength and consequently higher spatial resolution [6]. Recent work on phase matching of higher harmonics driven by IR pulses [12,13] have pointed out that for longer-wavelength driver pulses favorable phase matching conditions might be achievable that could mitigate the unfavorable $\lambda^{-5.5}$-scaling of the HHG efficiency in single-atom response. Thus, HHG driven by intense few-cycle IR pulses represents a promising route towards bright coherent X-ray sources with up to keV photon energies.

The main objective of our work is to generate IR pulses with ~40-fs duration that fully satisfy the requirements for external spectral broadening in gas [14]. In addition, with an IR pulse we expect to surpass the energy limitation (4-5 mJ at 0.8 µm) for gas broadening schemes because the critical power of self-focusing also scales as λ^2.

Using mJ pulses from Ti:sapphire amplifiers at 0.8 µm, coherent X-rays in the keV photon energy range were generated by HHG in helium [15]. A technological problem hindering further progress is gas ionization in the gas-filled hollow-fiber compressors required to achieve few-cycle pulse duration at pulse energies >1 mJ. More fundamentally, helium already saturates for intensities >1 PW/cm^2 and few-cycle pulses at 0.8 µm, thus the HHG cutoff and photon flux is limited by ground-state depletion in helium in these experiments.

Here, we report on the development of a multi-mJ all-optically synchronized and phase-stable OPCPA at 1.5 µm [16,17]. As opposed to our OPCPA system developed earlier [7], in this work we pursue a novel technological route: (1) with the advent of a mature 200-fs Yb MOPA system it became possible to abandon the Ti:sapphire front-end; (2) we avoid working close to the signal-idler wavelength degeneracy and reduce the quantum defect for the signal wave; (3) we employ (nearly) collinear Type-II phase matching that, as opposed to Type I, supports a much narrower bandwidth but is free of parasitic self-diffraction [18]. Following the pioneering work of Miller and coworkers [19,20], we employ Type-II KTP/KTA (1.030/1.064 µm pump, ~1.5 µm signal, ~3.5 µm idler) because these crystals are transparent for the mid-IR idler wavelength and exhibit a relatively broad bandwidth around 1.5 µm.

II. MULTIMILLIJOULE INFRARED FEW-CYCLE OPCPA

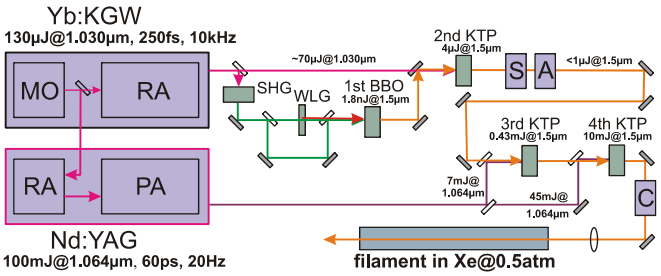

Fig.1. Scheme of the IR OPCPA setup. MO, master oscillator; RA, regenerative amplifier; PA, double-pass post amplifier; S/C grating-based stretcher/compressor; A, acousto-optic programmable dispersive filter (DAZZLER); WLG, white-light generator in a 10-mm-thick sapphire plate; the passively CEP-stable idler wave from stage 1 becomes the signal wave in stage 2. Stage 1 (Type-I BBO) is pumped at 515 nm, stage 2 (Type-II KTP) at 1.030 µm, stages 3 and 4 (Type-II KTP) at 1.064 µm.

978-1-4244-2906-6/08/$25.00 ©2008 IEEE

In our experimental scheme shown in Fig. 1, both Yb and Nd regenerative amplifiers (RA) are simultaneously seeded from a single master oscillator that has a modest FWHM bandwidth of 30 nm (see Fig. 2a). To seed the Nd RA, we pick up the zeroth-order diffraction beam behind a transmission grating in the pulse stretcher. The repetition rate of the Yb:KGW DPSS MOPA (Pharos, Light Conversion, Ltd.), tunable in the range of 1–100 kHz, was set at 10 kHz as the 500-th harmonic of the flash-lamp-pumped Nd:YAG amplifier (Ekspla Ltd.) operating at 20 Hz. In the Nd RA, an intracavity etalon is used to narrow the pulse bandwidth and make the pulse duration safe for post amplification (see Fig. 2b).

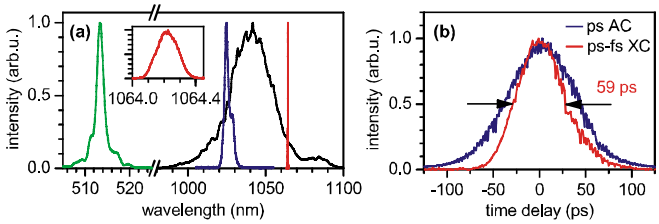

Fig.2. Optical synchronization of the Yb:KGW and Nd:YAG amplifiers. (a) Laser spectra: Kerr-lens mode-locked Yb:KGW oscillator (black), Yb:KGW regenerative amplifier (blue), Nd:YAG with an intracavity 2-mm-thick etalon (red), and SHG of Yb:KGW (green). (b) Pulse measurement of the ps Nd:YAG amplifier, showing an autocorrelation (AC) and a cross-correlation (XC) between the Yb:KGW (~200-fs) and Nd:YAG.

The 1.03 μm output from the femtosecond Yb:KGW MOPA is first split into two parts by means of a variable beam splitter (consisting of a half-waveplate and a thin-film polarizer); part one is used for implementing the 1st OPA stage, part two is used for pumping the 2nd OPA stage. In the 1st OPA stage, the 1.03 μm pulses are first frequency doubled in a 1-mm-thick Type-I BBO crystal (θ=23.4°, ϕ= 90°). Typically 8.5 μJ of 515 nm pulses are again split by a variable beam splitter into two parts: 1.3 μJ (measured behind a variable aperture used for fine-adjusting the input beam diameter) are focused onto a 10-mm-thick sapphire plate using an 87-mm focusing lens. In the sapphire plate, a stable white-light continuum extending to wavelengths >840 nm (see Fig. 3a) is created in a single filament. The white-light continuum, which is recollimated with a 40-mm lens, is used to seed the 1st OPA stage. The white-light seed pulses and the 515 nm pump pulses are combined collinearly (to avoid idler angular dispersion) on a dichroic beam splitter and both focused onto a 4-mm-thick Type-I BBO crystal (θ= 22.8°, ϕ=90°) with an f = 20 cm spherical mirror to a $1/e^2$ pump beam diameter of 120 μm. In the pump beam, a variable aperture is used to adjust the pump energy to 1.4 μJ (thus, the parametric gain) and to minimize the detrimental effects of amplified spontaneous emission. By adjusting both the θ-angle of the BBO crystal and time delay between the seed and pump pulses, different wavelength regions can be phase matched for efficient parametric amplification (Fig. 3a). In particular, selecting the ~795 nm wavelength for amplification, this configuration produces CEP-stable idler pulses [21] at 1.44 μm (Fig. 3b) that we use as seed in the 2nd OPA stage.

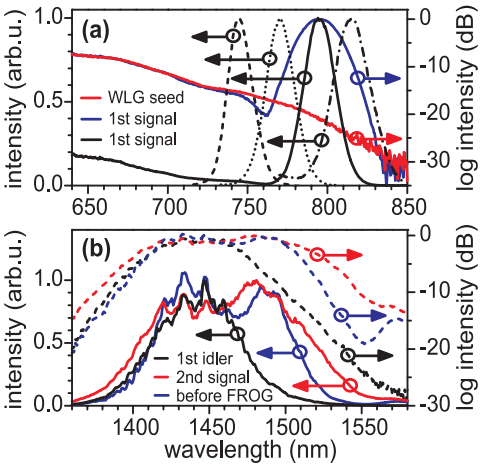

Fig. 3. Spectral properties of the 1st and 2nd OPA stages: NIR WLG seed (red) and signal spectra (blue and black solid) of the 1st OPA stage. The dashed and dotted curves indicate tunability of the 1st stage signal (and idler). (b) Infrared CEP-stable seed (black), amplified 2nd stage signal (red), spectrum measured before the FROG setup (blue).

For the amplification stages 2-4, we employ Type-II KTP/KTA crystals [19,20] (1.030/1.064 μm pump, ~1.5 μm signal, ~3.5 μm idler) because these crystals (unlike BBO, BIBO, and LBO) are transparent for the mid-IR idler wavelength and exhibit a relatively broad bandwidth around 1.5 μm. The CEP-stable idler pulses from the 1st OPA stage (i.e., the seed pulses for the 2nd OPA stage) are recollimated with a 10-cm lens and focused onto a 6-mm-thick Type-II KTP crystal (θ= 45.5°, ϕ=0°) using a 50-cm lens. The pump beam is focused onto the same KTP crystal using a 100-cm lens under an (external) walk-off compensation angle of 2.1° with respect to the seed beam. For a pump beam diameter of ~550 μm measured at the KTP crystal input face and 69 μJ (measured behind a variable aperture) pump pulses, we achieve a pump-signal conversion efficiency of ~5% in the 2nd OPA stage.

The strong nonlinear optical Kerr effect in KTP/KTA (nonlinear refractive index coefficient n_2(KTP/KTA) = 23.7 $\times 10^{16}$ cm^2/W as compared to n_2(BBO) = 2.9$\times 10^{16}$ cm^2/W [22]) raises the important question how severe is pump/idler-to-signal cross-phase modulation (XPM) in the 2nd OPA stage and its effect on CEP stability. The nonlinear effects accumulated during the OPA process in a nonlinear crystal of length L can be quantified by introducing a generalized B-integral

$$B = \frac{2\pi n_2}{\lambda_s}\int_0^L \mathrm{d}z\left[I_s(z) + \gamma_{sp} I_p(z) + \gamma_{si} I_i(z)\right] \qquad (1)$$

The coefficients γ_{sp} and γ_{si}, which quantify the pump-signal and idler-signal coupling, are 2 for parallel polarizations and 2/3 for orthogonal polarizations [23]. The resulting values of the coupling coefficients for the three types of phase matching in OPAs are summarized in Table I. Obviously, type II (o_s + e_i → e_p) phase matching as used in our amplification stages 2-4 minimizes the detrimental XPM contribution of pump and idler on the signal wave.

TABLE I

XPM COUPLING COEFFICIENTS γ_{sp} AND γ_{si}

phase-matching type	γ_{sp}	γ_{si}
type I ($o_s + o_i \rightarrow e_p$)	2/3	2
type II ($e_s + o_i \rightarrow e_p$)	2	2/3
type II ($o_s + e_i \rightarrow e_p$)	2/3	2/3

CEP stability of the 2nd OPA output was investigated by means of inline *f*-to-2*f* interferometry in the wavelength range from 650-790 nm (see Fig. 4). The observation of stable interference fringes directly proves CEP stability and negligible influence of XPM on the CEP. Note that OPCPA in the 3rd and 4th OPA stages preserve CEP stability of the seed pulses. The slow CEP drift observed in Fig. 4 is clearly of environmental origin and can easily be compensated for by feedback stabilization of the interferometer formed by the seed- and pump-paths in the 1st OPA stage (see Fig. 1).

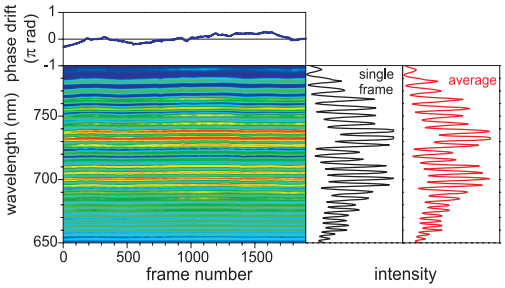

Fig. 4. *f*-to-2*f* interferogram exhibiting stable fringes due to CEP stability. The red and black curves on the right panels indicate the spectra averaged over 1900 frames (2 ms frame exposure time) and a single frame, respectively, on the same intensity axis. The blue curve in the above panel indicates the extracted phase drift of the 2nd stage signal.

This CEP-stable µJ-level two-stage OPA based on a DPSS femtosecond Yb-MOPA system represents an attractive alternative to traditional Ti:sapphire-based front-ends (e.g., [7-9]) for seeding multi-mJ OPCPA systems. In order to demonstrate this, the 2nd-stage signal pulses are stretched to ~40 ps and again recompressed to sub-40 fs duration using a grating-based stretcher/compressor pair [24] and an IR high-resolution acousto-optic programmable dispersive filter [25] (DAZZLER by Fastlite). Fig. 5 shows SHG-FROG measurements of 1.47-µm pulses with 92 nm FWHM bandwidth from the 2nd OPA stage after stretching to ~40 ps and recompression to a FWHM 33 fs pulse duration.

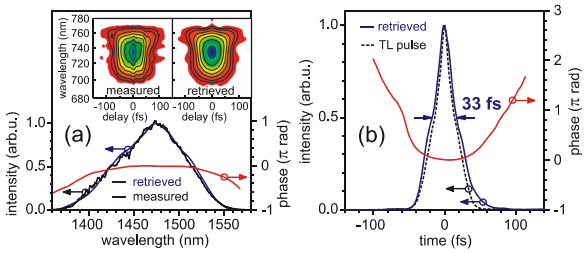

Fig. 5. SHG-FROG characterization of stretched and recompressed 1.47-µm pulses from the 2nd OPA stage: (a) Measured spectrum (black curve), retrieved spectral intensity (blue) and phase (red). The insets show the measured and retrieved FROG traces. (b) Retrieved temporal intensity (blue) and phase (red) profile indicating a FWHM 33 fs pulse duration. The transform-limited intensity profile (black dashed) corresponds to a 28 fs duration.

The temporally stretched 2nd-stage signal (i.e., the 3rd-stage seed) is amplified in two final OPCPA stages (3rd and 4th) using a 90-mJ picosecond pump pulse from the Nd:YAG system (Fig. 6a). The maximum energy of the signal pulses at 1.55 µm before recompression is ~10 mJ. As the output from the 4th OPA stage exhibits a spectral bandwidth comparable to the 2nd OPA stage (Fig. 5a), we are confident that the multi-mJ-level output from the power-amplification stages is recompressible to comparable pulse durations.

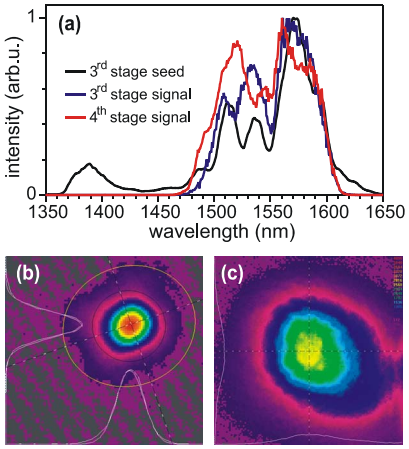

Fig. 6. (a) Spectral properties of the power amplification stages: spectrum of the 3rd stage seed (black curve), and amplified signal spectra after the 3rd (blue) and 4th (red) amplification stages. (b) Far-field beam profile of the 2nd-stage signal wave. (c) Beam profile of the multi-mJ signal wave after 5× magnification with a Galilean beam expander before recompression.

The $1/e^2$-beam diameter of the 4th-stage output is widened by a factor of 5 to 9.5 mm by means of a Galilean beam expander in order to avoid damaging of the gold grating in the compressor.

III. FILAMENTATION IN XENON

After recompressing the 4th-stage signal pulses we performed a preliminary filamentation experiment (Fig. 7).

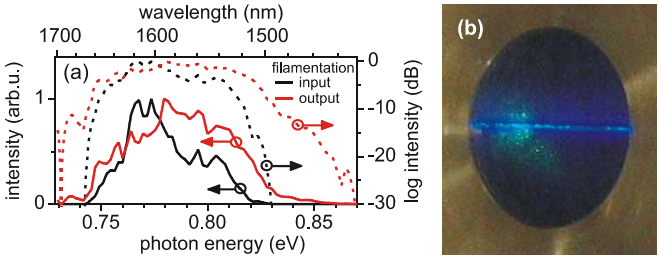

Fig. 7: Filamentation of recompressed 1.4-mJ 1.57-µm pulses in xenon at 0.5 atm: (a) Input (black curve) and output spectra (red) of the filamentation experiment on a linear and logarithmic scale, respectively. (b) Filament observed through the output window.

In this first experiment, we only used 1.4-mJ pulses at 1.6 µm in order to ensure a single filament under the current experimental conditions. These pulses are focused into a 43-cm long gas cell filled with xenon (12.13 eV ionization potential) at 0.5 atm pressure using a 40-cm lens placed ~25 cm in front of the gas cell. The input window of the cell has

an antireflection coating covering the input pulse spectrum, the output window is a standard BK7 window. The preliminary results shown in Fig. 7a exhibit noticeable spectral broadening. Through the output window of the xenon cell, a narrow single filament can be observed due to the fifth harmonic generated in the filament (blue light in Fig. 7b).

IV. Conclusions and Outlook

In conclusion, we have demonstrated 10-mJ CEP-stable parametric amplification at ~1.5 μm based on a merger of a DPSS femtosecond Yb-MOPA system and picosecond Nd:YAG solid-state technology. In a first preliminary filamentation experiment, we have observed spectral broadening of the recompressed output from the 4-stage parametric amplifier. Current work aims to optimize the recompression of the 20-Hz multi-mJ output pulses and the filamentation with respect to spectral broadening and energy throughput by varying the parameters pulse energy and chirp, beam diameter, focusing, gas type and pressure. Ultimately, with an IR pulse we expect to surpass the energy limitation (4-5 mJ at 800 nm) for gas broadening schemes because the critical power of self-focusing scales as λ^2.

Acknowledgment

This work is supported by the Austrian Science Fund (FWF), grants U33-N16 and F1619-N08. O. D. Mücke gratefully acknowledges support from a Lise-Meitner Fellowship by the FWF under project number M1094-N14.

References

[1] A. Dubietis, R. Butkus, A. P. Piskarskas, "Trends in chirped pulse optical parametric amplification," *IEEE J. Sel. Topics Quantum Electron.*, vol. 12, pp. 163-172, 2006; and references therein.

[2] M. Hentschel, R. Kienberger, C. Spielmann, G. A. Reider, N. Milosevic, T. Brabec, P. Corkum, U. Heinzmann, M. Drescher, and F. Krausz, "Attosecond metrology," *Nature*, vol. 414, pp. 509-513, 2001.

[3] R. Kienberger, E. Goulielmakis, M. Uiberacker, A. Baltuska, V. Yakovlev, F. Bammer, A. Scrinzi, T. Westerwalbesloh, U. Kleineberg, U. Heinzmann, M. Drescher, and F. Krausz, "Atomic transient recorder," *Nature*, vol. 427, 817-821, 2004.

[4] G. Sansone, E. Benedetti, F. Calegari, C. Vozzi, L. Avaldi, R. Flammini, L. Poletto, P. Villoresi, C. Altucci, R. Velotta, S. Stagira, S. De Silvestri, and M. Nisoli, "Isolated Single-Cycle Attosecond Pulses," *Science*, vol. 314, 443-446, 2006.

[5] J. Itatani, J. Levesque, D. Zeidler, H. Niikura, H. Pépin, J. C. Kieffer, P. B. Corkum, and D. M. Villeneuve, "Tomographic imaging of molecular orbitals," *Nature*, vol. 432, 867-871, 2003.

[6] M. Meckel, D. Comtois, D. Zeidler, A. Staudte, D. Pavicic, H. C. Bandulet, H. Pépin, J. C. Kieffer, R. Dörner, D. M. Villeneuve, and P. B. Corkum, "Laser-Induced Electron Tunneling and Diffraction," *Science*, vol. 320, pp. 1478-1482, 2008; and references therein.

[7] T. Fuji, N. Ishii, C. Y. Teisset, X. Gu, Th. Metzger, A. Baltuska, N. Forget, D. Kaplan, A. Galvanauskas, and F. Krausz, "Parametric amplification of few-cycle carrier-envelope phase-stable pulses at 2.1 μm," *Opt. Lett.*, vol. 31, pp. 1103-1105, 2006.

[8] C. Vozzi, G. Cirmi, C. Manzoni, E. Benedetti, F. Calegari, G. Sansone, S. Stagira, O. Svelto, S. De Silvestri, M. Nisoli, and G. Cerullo, "High-energy, few-optical-cycle pulses at 1.5 μm with passive carrier-envelope phase stabilization," *Opt. Express*, vol. 14, pp. 10109-10116, 2006.

[9] C. Vozzi, F. Calegari, E. Benedetti, S. Gasilov, G. Sansone, G. Cerullo, M. Nisoli, S. De Silvestri, and S. Stagira., "Millijoule-level phase-stabilized few-optical-cycle infrared parametric source," *Opt. Lett.*, vol. 32, pp. 2957-2959, 2007.

[10] J. Tate, T. Auguste, H. G. Muller, P. Salières, P. Agostini, and L. F. DiMauro, "Scaling of Wave-Packet Dynamics in an Intense Midinfrared Field," *Phys. Rev. Lett.*, vol. 98, pp. 013901-1-4, 2007.

[11] P. Colosimo, G. Doumy, C. I. Blaga, J. Wheeler, C. Hauri, F. Catoire, J. Tate, R. Chirla, A. M. March, G. G. Paulus, H. G. Muller, P. Agostini, and L. F. DiMauro, "Scaling strong-field interactions towards the classical limit," *Nature Phys.*, vol. 4, pp. 386-389, 2008; and references therein.

[12] V. S. Yakovlev, M. Ivanov, and F. Krausz, "Enhanced phase-matching for generation of soft X-ray harmonics and attosecond pulses in atomic gases," *Opt. Express*, vol. 15, pp. 15351-15364, 2007.

[13] T. Popmintchev, M.-C. Chen, O. Cohen, M. E. Grisham, J. J. Rocca, M. M. Murnane, and H. C. Kapteyn, "Extended phase matching of high harmonics driven by mid-infrared light," *Opt. Lett.*, vol. 33, 2128-2130, 2008.

[14] P. Hauri, R. B. Lopez-Martens, C. I. Blaga, K. D. Schultz, J. Cryan, R. Chirla, P. Colosimo, G. Doumy, A. M. March, C. Roedig, E. Sistrunk, J. Tate, J. Wheeler, L. F. DiMauro, and E. P. Power, "Intense self-compressed, self-phase-stabilized few-cycle pulses at 2 μm from an optical filament," *Opt. Lett.*, vol. 32, pp. 868-870, 2006.

[15] J. Seres, E. Seres, A. J. Verhoef, G. Tempea, C. Streli, P. Wobrauschek, V. Yakovlev, A. Scrinzi, C. Spielmann, F. Krausz, "Source of coherent kiloelectronvolt X-rays," *Nature*, vol. 433, p. 596, 2005.

[16] O. D. Mücke, D. Sidorov, P. Dombi, A. Pugžlys, A. Baltuška, S. Ališauskas, V. Smilgevičius, J. Pocius, L. Giniūnas, R. Danielius, and N. Forget, "Scalable Yb-MOPA-Driven Carrier-Envelope Phase-Stable Few-Cycle Parametric Amplification at 1.5 μm," *Opt. Lett.*, in press.

[17] O. D. Mücke, D. Sidorov, P. Dombi, A. Pugžlys, A. Baltuška, S. Ališauskas, J. Pocius, L. Giniūnas, and R. Danielius, in *Ultrafast Phenomena XVI*, P. Corkum, K. Nelson, E. Riedle, R. Schoenlein, and S. De Silvestri, Eds., Springer, Berlin, in press.

[18] A. Varanavičius, A. Dubietis, A. Beržanskis, R. Danielius, and A. Piskarskas, "Near-degenerate cascaded four-wave mixing in an optical parametric amplifier," *Opt. Lett.*, vol. 22, pp. 1603-1605, 1997.

[19] D. Kraemer, R. Hua, M. L. Cowan, K. Franjic, and R. J. D. Miller, "Ultrafast noncollinear optical parametric chirped pulse amplification in $KTiOAsO_4$," *Opt. Lett.*, vol. 31, pp. 981-983, 2006.

[20] D. Kraemer, M. L. Cowan, R. Hua, K. Franjic, and R. J. D. Miller, "High-power femtosecond infrared laser source based on noncollinear optical parametric chirped pulse amplification," *J. Opt. Soc. Am. B*, vol. 24, pp. 813-818, 2007.

[21] A. Baltuška, T. Fuji and T. Kobayashi, "Controlling the carrier-envelope phase of ultrashort light pulses with optical parametric amplifiers," *Phys. Rev. Lett.*, vol. 88, 133901-1-4, 2002.

[22] W. Koechner, *Solid-State Laser Engineering*, 6th edition, Springer, Berlin, 2006.

[23] G. P. Agrawal, *Nonlinear Fiber Optics*, 4th edition, Academic Press, New York, 2007

[24] M. P. Kalashnikov, E. Risse, H. Schönnagel, and W. Sandner, "Double chirped-pulse-amplification laser: a way to clean pulses temporally," *Opt. Lett.*, vol. 30, pp. 923-925, 2005

[25] F. Verluise, V. Laude, J.-P. Huignard, P. Tournois, and A. Migus, "Arbitrary dispersion control of ultrashort optical pulses with acoustic waves," *J. Opt. Soc. Am. B*, vol. 17, pp. 138-145, 2000.